Disruption of the NF-H Gene Increases Axonal Microtubule Content and Velocity of Neurofilament Transport: Relief of Axonopathy Resulting from the Toxin β,β′-Iminodipropionitrile

Qinzhang Zhu, Michael Lindenbaum, Françoise Levavasseur, Hélène Jacomy, and Jean-Pierre Julien

Centre for Research in Neuroscience, McGill University, The Montreal General Hospital Research Institute, Montréal, Québec, Canada H3G 1A4

Abstract. To investigate the role of the neurofilament heavy (NF-H) subunit in neuronal function, we generated mice bearing a targeted disruption of the gene coding for the NF-H subunit. Surprisingly, the lack of NF-H subunits had little effect on axonal calibers and electron microscopy revealed no significant changes in the number and packing density of neurofilaments made up of only the neurofilament light (NF-L) and neurofilament medium (NF-M) subunits. However, our analysis of NF-H knockout mice revealed an ~2.4-fold increase of microtubule density in their large ventral root axons. This finding was further corroborated by a corresponding increase in the ratio of assembled tubulin to NF-L protein in insoluble cytoskeletal preparations from the sciatic nerve. Axonal transport studies carried out by the injection of [^{35}S]methionine into spinal cord revealed an increased transport velocity of newly synthesized NF-L and NF-M proteins in motor axons of NF-H knockout mice. When treated with β,β′-iminodipropionitrile (IDPN), a neurotoxin that segregates microtubules and retards neurofilament transport, mice heterozygous or homozygous for the NF-H null mutation did not develop neurofilamentous swellings in motor neurons, unlike normal mouse littermates. These results indicate that the NF-H subunit is a key mediator of IDPN-induced axonopathy.

Key words: neurofilament • axon caliber • microtubules • iminodipropionitrile • gene targeting

Neurofilaments are made up by the copolymerization of three intermediate filament proteins, neurofilament light (NF-L)[1] (61 kD), neurofilament medium (NF-M) (90 kD), and neurofilament heavy (NF-H) (110 kD) (Hoffman and Lasek, 1975; Liem et al., 1978). In the mouse, neurofilaments are obligate heteropolymers requiring NF-L with either NF-M or NF-H for polymer formation (Ching and Liem, 1993; Lee et al., 1993). A remarkable feature of the NF-H protein is its long COOH-terminal tail domain that forms side-arm projections at the periphery of the filament. The tail NF-H domain is rich in charged amino acids and has multiple repeats Lys-Ser-Pro (KSP) that account for its unusual high content of phosphoserine residues (Julien and Mushynski, 1982; Carden et al., 1985; Julien et al., 1988; Lees et al., 1988). The presence of charged amino acids in NF-M and NF-H led to the suggestion that repulsive forces between neurofilaments would affect neurofilament packing density and axonal caliber. Evidence for this notion has come from studies on the dysmyelinating mutant *Trembler* mouse (deWaegh et al., 1992) and on hypomyelinating transgenic mice expressing in Schwann cells either a diphtheria toxin A or SV-40 large T antigen in which reduced levels of NF-H phosphorylation resulted in decreases in axon caliber (Cole et al., 1994). In addition, there is evidence that the NF-H protein may act as a modulator of axonal transport. The appearance of NF-H protein during postnatal development coincides with slowing of axonal transport (Willard and Simon, 1983), whereas overexpression of either human or mouse NF-H proteins in transgenic mice cause an impairment of neurofilament transport (Collard et al., 1995; Marszalek et al., 1996). The precise mechanism by which NF-H overexpression can reduce neurofilament transport remains unknown.

The abnormal accumulations of neurofilaments in distinct regions of the neuron occur in a variety of disorders including amyotrophic lateral sclerosis (ALS) (Carpenter, 1968; Hirano et al., 1984; Chou, 1992), an inherited giant axonal neuropathy in children (Carpenter et al., 1974), and toxic neuronopathies induced by, 2,5-hexanedione (Graham et al., 1984), acrylamide (Asbury and Johnson, 1978),

1. *Abbreviations used in this paper*: ALS, amyotrophic lateral sclerosis; DRG, dorsal root ganglia; ES, embryonic stem; IDPN, β,β′-iminodipropionitrile; NF-H/NF-L/NF-M, neurofilament heavy/neurofilament light/neurofilament medium.

Address all correspondence to Jean-Pierre Julien, The Montreal General Hospital Research Institute, 1650 Cedar Avenue, Montréal, Québec, Canada H3G 1A4. Tel.: (514) 937-6011 ext. 2361. Fax: (514) 934-8265. E-mail: mdju@musica.mcgill.ca

aluminium (Troncoso, 1992), and β,β′-iminodipropionitrile (IDPN) (Griffin et al., 1978). The pathology in the case of IDPN is of particular interest because this agent induces abnormal neurofilamentous accumulations in proximal axons similar to those found in ALS (Griffin et al., 1978). The molecular mechanism underlying IDPN-mediated pathology remains unknown but it is well established that IDPN intoxication causes segregation of neurofilaments from microtubules. Increases in immunoreactivity of NF-H phosphorylation-related epitopes have been reported after IDPN treatment (Watson et al., 1989). However, during the early phase of IDPN intoxication a transient dephosphorylation of NF-H precedes an increase in the proportion of cold-soluble tubulin and the formation neurofilament accumulations. These early changes suggested a role for the NF-H protein in modulating neurofilament-microtubule interactions and perhaps microtubule stabilization (Tashiro et al., 1994).

To further investigate the role of NF-H in neuronal function and in toxin-induced axonopathy, we generated mice bearing a targeted disruption of the NF-H gene using the technique of homologous recombination in embryonic stem cells. We report here that the absence of NF-H had no significant effect on neurofilament formation but it resulted in higher microtubule density in large motor axons and it increased velocity of neurofilament transport. Moreover, IDPN treatment of mice homozygous or heterozygous for the NF-H null mutation revealed that the NF-H protein is a key mediator of axonopathy induced by this agent.

Materials and Methods

Targeting Vector

The mouse genomic NF-H DNA was isolated from a mouse phage genomic library as described previously (Julien et al., 1988). The targeting vector was constructed by insertion of a blunt-ended 1.1-kb XhoI and BamHI fragment of pMC1neoPoly A (Stratagene, La Jolla, CA) into the second XmaI site of the NF-H gene as shown in the Fig. 1 *A*. The final targeting fragment was excised out by BamHI digestion and then purified by b-Agarase (GIBCO BRL, Gaithersburg, MD).

Cell Culture, Embryo Microinjection, and Animal Breeding

The culture of R1 embryonic stem (ES) cells (a gift from J. Roder, Mount Sinai Research Institute, Toronto, Canada) and transfection were carried out as previously described (Mansour et al., 1988; Ramirez-Solis et al., 1993). ES cells (10^7) were transfected with 25 mg of purified targeting DNA using the BRL Cell Porator at 330 mF 230 V in DME at room temperature. The cells were treated with 180 mg/ml of G418 at 24 h after electroporation for 3 d, and then the concentration of G418 was increased to 360 mg/ml. After 7–8 d under G418 selection, colonies were picked up, trypsinized, and then plated onto 96-well plates with SNL feeder layer (feeder layer and LIF 1,000 units/ml were used all time in the ES cell culture). Cells were trypsinized 4 d later and 30% of the cells were plated for DNA extraction onto gelatin-coated 96-well plates while 70% of them were frozen in duplicate plates. DNA was extracted after 5 d of culture and digested with EcoRI in the plates (Ramirez-Solis et al., 1993). The ES cell clones that yielded an expected 2.8-kb recombinant band on Southern blot (see Fig. 1) were expanded and reprobed by Neo probe to exclude the clones with random insertions. Three ES cell clones were injected into C57BL/6 blastocysts as described before (Mansour et al., 1988). Germline transmission was obtained by mating male chimeras with C57BL/6 females. The use of animals and all surgical procedures described in this article were carried out according to The Guide to the Care and Use of Experimental Animals of the Canadian Council on Animal Care (see http://www.pharma.mcgill.ca/grant.htm).

RNA Analysis

Mice were killed by pentobarbital overdose and tissue samples were immediately frozen after dissection in liquid nitrogen and stored at −80°C. Total RNA was isolated by homogenization in guanidinium thiocyanate according to the method of Chomczynski and Sacchi (1987). The RNA samples (20 mg) were fractionated on a 1% agarose–formaldehyde gel before blotting on a Hybond N^+ membrane (Amersham Corp., Arlington Heights, IL). The DNA probes were labeled with [α-^{32}P]dATP by random priming. Hybridizations were performed for 16 h at 42°C in 50% formamide, 1 M NaCl, 50 mM Tris, pH 7.5, 0.2% Ficoll, 0.2% polyvinyl pyrrolidone, 0.1% sodium pyrophosphate, 1% SDS, and 100 mg/ml sonicated and denatured salmon sperm DNA. Blots were washed in 2× SSC–0.1% SDS at room temperature for 10 min, in 2× SSC–0.1% SDS at 65°C twice for 10 min, and in 0.5× SSC–0.1% SDS at room temperature once for 15 min. Blots were exposed to film (X-OMat AR; Eastman Kodak, Rochester, NY) with intensifying screens for 18 h at −80°C.

Western Blot Analysis

The mice were killed by intra-peritoneal injection of overdose pentobarbital and the nervous tissue samples were frozen in liquid nitrogen and stored at −80°C. Total protein extracts were obtained by homogenization of samples in SDS–urea buffer (0.5% SDS, 8 M urea in 7.4 phosphate buffer). The supernatant was collected after centrifugation at 10,000 *g* for 20 min. The protein concentration was estimated by the Bradford procedure (Bio-Rad Laboratories, Hercules, CA). The proteins (10 mg) were fractionated on a 7.5% SDS-PAGE and either visualized by Coomassie blue staining or blotted onto a nitrocellulose membrane for Western blot analysis. The mAbs against NF-L and NF-H were purchased from Amersham Corp. and Sternberger Inc. (Lutherville, MD), respectively. The mAbs against tau, tubulin, and actin were purchased from Boehringer Mannheim Corp. (Indianapolis, IN). The mAb against acetylated tubulin was purchased from Sigma Chemical Co. (St. Louis, MO). The Western blot results were revealed by Renaissance® (a Western blot chemiluminescence kit from Dupont-NEN™, Boston, MA).

IDPN Intoxication

Five sets of 2–3-mo-old NF-H +/+, NF-H +/−, and NF-H −/− littermates were intoxicated with two doses (first day and fifth day) of IDPN intraperitoneally (1.5 g/kg body weight in 50% saline solution; Aldrich Chemical Co., Milwaukee, WI) and maintained on 0.02% IDPN in drinking water. IDPN-treated mice were analyzed at 0, 7, and 15 d after intoxication.

Histological Methods

Mice were killed by overdose of pentobarbital, perfused with 0.9% NaCl, and then with fixative (2.5% glutaraldehyde, 0.5% PFA in 0.1 M sodium phosphate buffer, pH 7.4). Tissue samples were immersed in fixative for 2 h, rinsed in phosphate buffer, and then postfixed in 1% phosphate buffered osmium tetroxide. After three washes with phosphate buffer, each sample was dehydrated in a graded series of ethanol and embedded in Epon. The thin sections were stained with Toluidine blue and examined under a Polyvar microscope. The counting of axons and evaluation of myelin thickness in the L5 ventral root were carried out with the Image-1 software from Universal Imaging Corporation (West Chester, PA). The ultrathin sections were stained with lead citrate and examined with a Philips CM10 electron microscope (Philips Electron Optics, Mahwah, NJ).

Ultrastructural Morphometry Analysis

Ultrathin cross sections (100 nm) of L5 ventral root axons (>5 mm in diam) at the dorsal root ganglia (DRG) region were photographed at a magnification of 11,500× and enlarged to a final magnification of 81,650× by printing. Positions of 10-nm filaments were marked by puncturing the print with a needle, and then captured by a CCD camera and digitized using Imagine I. Digitized x-y coordinates were then computed by an IBM program written in C++ programming language. Nearest neighbor distance was calculated for each filament. Neurofilament packing density was calculated using the tile-counting procedure as previously reported (Hsieh et al., 1994) with the following modifications. Square tiles of 100 nm × 100 nm were used, and tiles that did not contain any end-on neurofilaments were eliminated by the program.

The density and distribution of microtubules vary substantially according to the type of neurons, axonal caliber size, and myelination status of the axon (Hsieh et al., 1994). Analysis of microtubules was carried out as follows. Ultrathin cross sections (100 nm) of L5 ventral root axons of 5.0–5.5 mm in diameter at the level of DRG region having a clear myelin sheath were photographed at a magnification of 3,100× and enlarged another 8 times by printing. The position of 25-nm microtubules were taken in the same way as described above for neurofilament calculation. Axon area for the density calculation did not include myelin sheath. All calculations were done by a computer program with a graphic display written specifically for this application.

Taxol-stabilized Microtubule Preparations

Sciatic nerves between DRG and obturator tendon were dissected out from newly killed mice and homogenized in a 2-ml glass-to-glass tissue grinder in 1 ml of taxol/Triton X-100 PHEM extraction medium (60 mM Pipes, 25 mM Hepes, 10 mM EGTA, 2 mM MgCl, 0.1% DMSO 10 μg/ml leupeptin, and 0.6 mM PMSF) (Black et al., 1986). The homogenates were incubated at room temperature for 30 min to solubilize unassembled tubulin and then centrifuged for 45 min in a Beckman TLA 45 rotor at 30,000 rpm. The pellets were dissolved in 100 μl of 1% SDS-Tris buffer (50 mM Tris, pH 7.4) and the protein content was estimated by the Bio-Rad Dc Protein Assay kit (Bio-Rad Modified Lowry method). The proteins (10 μg) were fractionated on a 7.5% SDS-PAGE and either visualized by Coomassie blue staining or blotted on a nitrocellulose membrane for Western blot analysis. Densitometric analysis was carried out by the GelPro™ Analyzer (version 2.0) from Meia cybernetics (Silver Spring, MD).

Metabolic Labeling

Proteins carried by slow axonal transport in sciatic motor axons were metabolically labeled and fractionated mainly as previously reported (Kirkpatrick and Brady, 1994). Aliquots of 0.5 mCi of [^{35}S]methionine (DuPont-NEN) in 1-ml vol were injected into the anterior horn area of L2-L4 spinal cord twice on each side, 1-mm deep from the dorsal surface and 1 mm from the middle groove at a rate of 0.05 ml/min. 30 d after labeling, the sciatic nerves with ventral roots (L3 to L5) were dissected out from both sides and cut into 3-mm consecutive segments. Proteins were fractionated by SDS-PAGE and radiolabeled proteins detected by fluorography.

Results

Targeted Disruption of NF-H Gene in Mice

A genomic fragment of NF-H was isolated from a mouse library using a mouse cDNA probe (Julien et al., 1986). The mouse NF-H gene contains four exons separated by three introns (Julien et al., 1988). A targeting vector of ~8

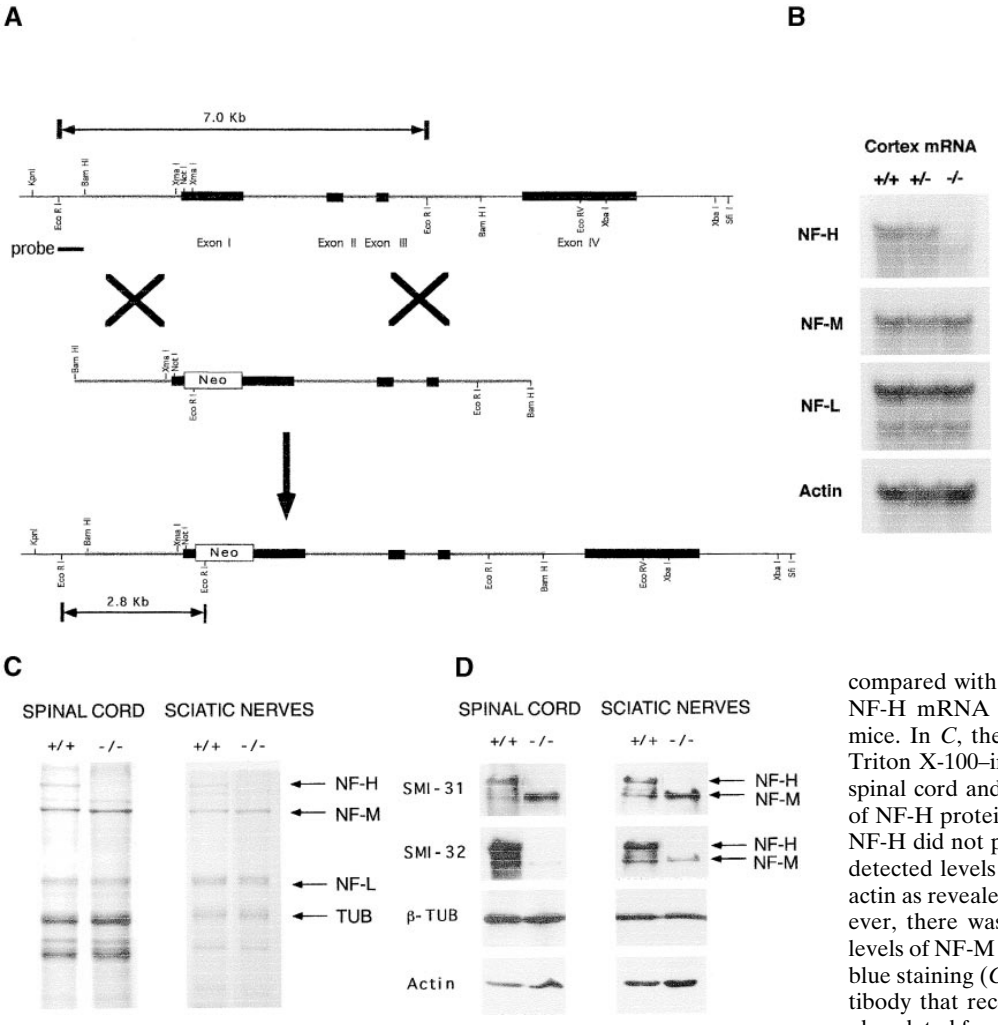

Figure 1. Targeted disruption of the NF-H gene. *A* shows the restriction map of the mouse genomic NF-H and targeting vector. The targeting vector was generated by inserting a 1.1-kb *Neo* cassette from pMC1NEOpolyA into the second XmaI site of a BamHI/BamHI NF-H fragment of ~8 kb. The EcoRI/BamHI fragment of the 5′ end was used as a probe for Southern blotting to detect a 2.8-kb EcoRI fragment indicative of homologous recombination. As shown in *B*, no changes in the levels of mRNA for NF-M and NF-L were detected in the brain of NF-H heterozygous (+/−) and homozygous (−/−) mutant mice. The levels of NF-H mRNA decreased by ~50% in NF-H +/− mice as compared with +/+ littermate. As expected, no NF-H mRNA was detected in the NF-H −/− mice. In *C*, the Coomassie blue–stained gels of Triton X-100–insoluble extracts at 4°C from the spinal cord and sciatic nerve confirmed the lack of NF-H protein in NF-H −/− mice. The loss of NF-H did not provoke significant changes in the detected levels of NF-L (*C*) or of β-tubulin and actin as revealed by the immunoblots in *D*. However, there was a modest increase of ~20% in levels of NF-M protein as detected by Coomassie blue staining (*C*). As shown in *D*, the SMI-31 antibody that recognizes primarily the hyperphosphorylated form of NF-H in normal mice yielded a dramatic increase of ~10-fold in reactivity for the NF-M band in samples from NF-H null mice. This is likely the reflect of a compensatory increase in phosphorylation state of NF-M protein that contains, like NF-H, multiple Lys-Ser-Pro phosphorylation sites.

kb was constructed by inserting a *TK/Neo* cassette into the XmaI site of exon I as shown in Fig. 1 *A*. The DNA fragment was transfected by electroporation into R1 ES cells and neomycin resistance colonies were selected (Nagy et al., 1993). A total of 288 G418-resistant clones were picked up. Three ES cell clones out of eleven selected for homologous recombination event were microinjected into mouse blastocysts to generate chimeric mice. The majority of chimeras derived from this ES cell line were males and they were able to transmit agouti coat color to their progeny when mated to C57BL/6 females. About half of agouti progeny (F1) were heterozygous for the NF-H null mutation. The genotype of the mice was determined by Southern blot analysis of tail DNA. A Mendelian transmission of the NF-H disrupted gene was obtained by the breeding of heterozygous NF-H +/− F1 males and females. Thus, the NF-H null mutation in mice does not cause lethality during embryonic development or after birth. The homozygous NF-H knock-out mice were fertile and appeared phenotypically normal.

Levels of NF-L and NF-M in the Absence of NF-H

Northern blot analysis was carried out with 10 μg of total brain mRNA of adult NF-L +/+, +/−, and −/− mice (Fig. 1 *B*). No NF-H mRNA was detected in NF-H knockout mice while ~50% decrease in NF-H mRNA was detected in NF-H heterozygous +/− mice. The depletion of NF-H mRNA did not affect the level of expression of either NF-M or NF-L mRNAs. Coomassie blue–stained gels of Triton X-100–insoluble extracts at 4°C from the spinal cord and sciatic nerve showed absence of NF-H protein in NF-H −/− mice (Fig. 1 *C*). This was further confirmed by immunoblotting (Fig. 1 *D*). No band corresponding to NF-H was detected with SMI-31 and SMI-32 antibodies (Sternberger Inc.) that recognizes the hyperphosphorylated and hypophosphorylated forms of NF-H, respectively. The lack of NF-H protein did not affect the levels of NF-L protein but it resulted in a modest increase of ~20% in NF-M levels (Fig. 1 *C*). Thus, unlike the situation with NF-L knockout mice where dramatic decreases in the levels of both NF-M and NF-H proteins were observed (Zhu et al., 1997), the absence of NF-H did not cause dramatic changes on the stability of the other two neurofilament subunits, NF-M and NF-L. However, it is noteworthy that the loss of NF-H protein increased dramatically the signal of NF-M cross-reactivity with the SMI-31 antibody (Fig. 1 *D*). This is likely due to a compensatory increase in the phosphorylation state of NF-M that contains, like NF-H, multiple Lys-Ser-Pro phosphorylation sites (Levy et al., 1987; Myers et al., 1987).

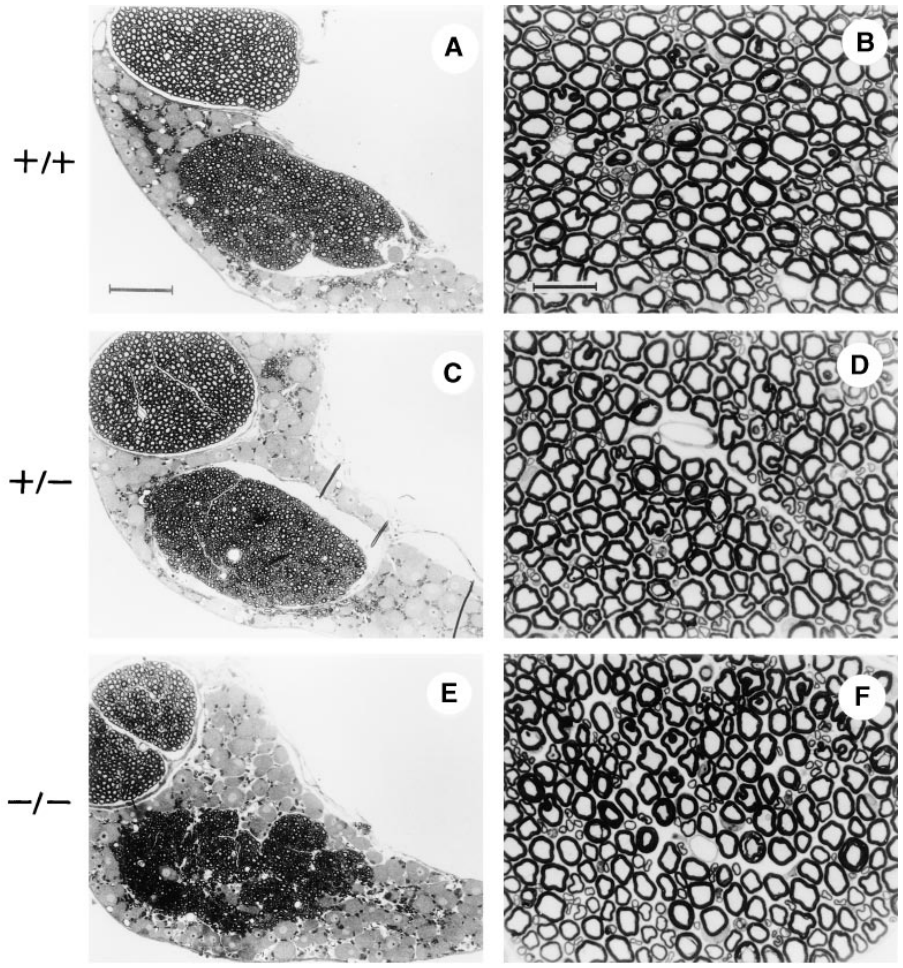

Figure 2. Light microscopy of peripheral myelinated axons. The lack of NF-H subunit in +/− and −/− mice had little effects on the caliber of axons from DRG neurons (*A*, *C*, *E*) or from L5 ventral roots (*B*, *D*, *F*). Bar: (*A*, *C*, *E*) 100 μm; (*B*, *D*, *F*) 20 μm.

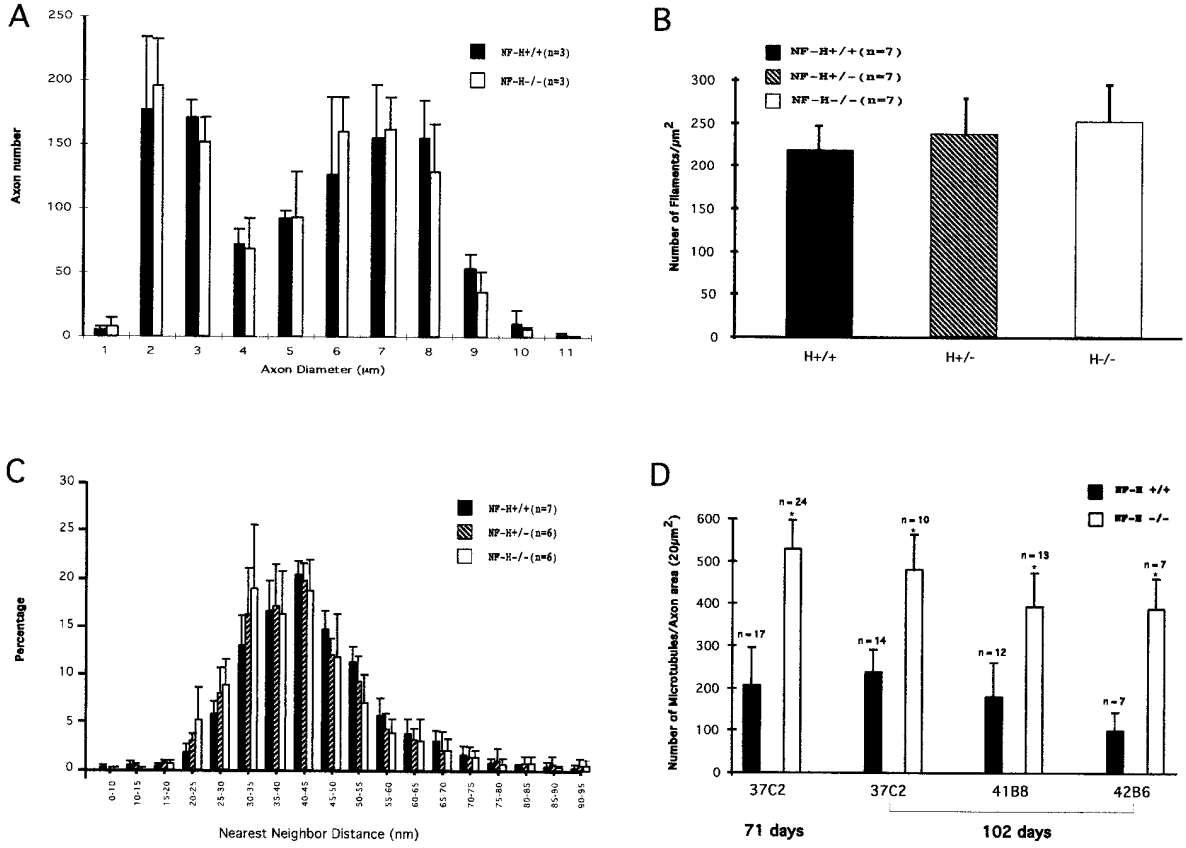

Figure 3. Cytoskeletal changes in L5 ventral root axons lacking NF-H. Comparison of axonal calibers (*A*), neurofilament content (*B*), and nearest neighbor distances (*C*), and density of microtubules in L5 ventral root axons from NF-H +/+, NF-H +/−, and NF-H −/− mice. The *n* (*A*) represents the number of animals and results were obtained from three sets of littermates age of 71 and 100 d. The results in *B* and *C* were derived from 71-d-old littermates. The most remarkable cytoskeletal change in the absence of NF-H was the dramatic increase (∼2.4-fold) in the density of microtubules. The data in *D* were derived from four NF-H knockout mice obtained from three independent ES cell lines called 37C2, 41B8, and 42B6. The age of the mice is shown at the bottom of the figures. The data show the mean ± SD. The *t* test was applied. $*P < 0.0001$.

No Substantial Changes in Density of Neurofilaments and in Calibers of Axons

Since there are some lines of evidence suggesting a role for NF-H protein in neurofilament spacing and axonal caliber (deWaegh et al., 1992; Hsieh et al., 1994; Nixon et al., 1994), light and electron microscopy was carried out on L5 ventral roots of adult NF-H +/+, NF-H +/−, and NF-H −/− mice. Surprisingly, the NF-H depletion caused only modest changes in the caliber of myelinated axons (Figs. 2 and 3 *A*). Like NF-H +/+ mice, the NF-H −/− mice yielded a bimodal distribution of axonal calibers representing the small and large myelinated axons (Fig. 3 *A*). In the NF-H −/− mice, the caliber of large myelinated axons was only slightly smaller (∼10%) than those of normal mice. To examine whether interfilament spacing was affected in large ventral root axons lacking NF-H, we recorded the positions of each filament in individual axons and calculated nearest neighbor distances for each neurofilament. No significant changes in the number of assembled neurofilaments were observed in NF-H +/− and NF-H −/− mice (Fig. 3 *B*). The NF-H subunit was clearly dispensable for the formation of 10-nm filaments and its absence caused no substantial changes in the average nearest neighbor distance, neurofilament packing density and axon caliber (Figs. 3 and 4).

Increased Density of Microtubules in Ventral Root Axons

The most remarkable change in the axonal cytoskeleton of ventral root axons lacking NF-H was a ∼2.4-fold increase in microtubule content (Fig. 3 *D*). Considering that the density and distribution of microtubules may vary according to the type of neurons, axonal caliber size, and myelination status of the axon (Hsieh et al., 1994), our analysis was carried out on large myelinated axons (∼20 mm^2 ± 2.5 axoplasmic area) of the L5 ventral root, a well-defined population of axons. We counted the number of microtubules on electron micrographs of individual transverse sections of axons magnified 25,000×. Our study involved four pairs of NF-H +/+ and NF-H −/− littermates with two sets derived from three distinct ES cell clones and, for each animal, 7–24 axons were analyzed. The number of microtubules per axonal area (20 mm^2) was of 193 ± 86

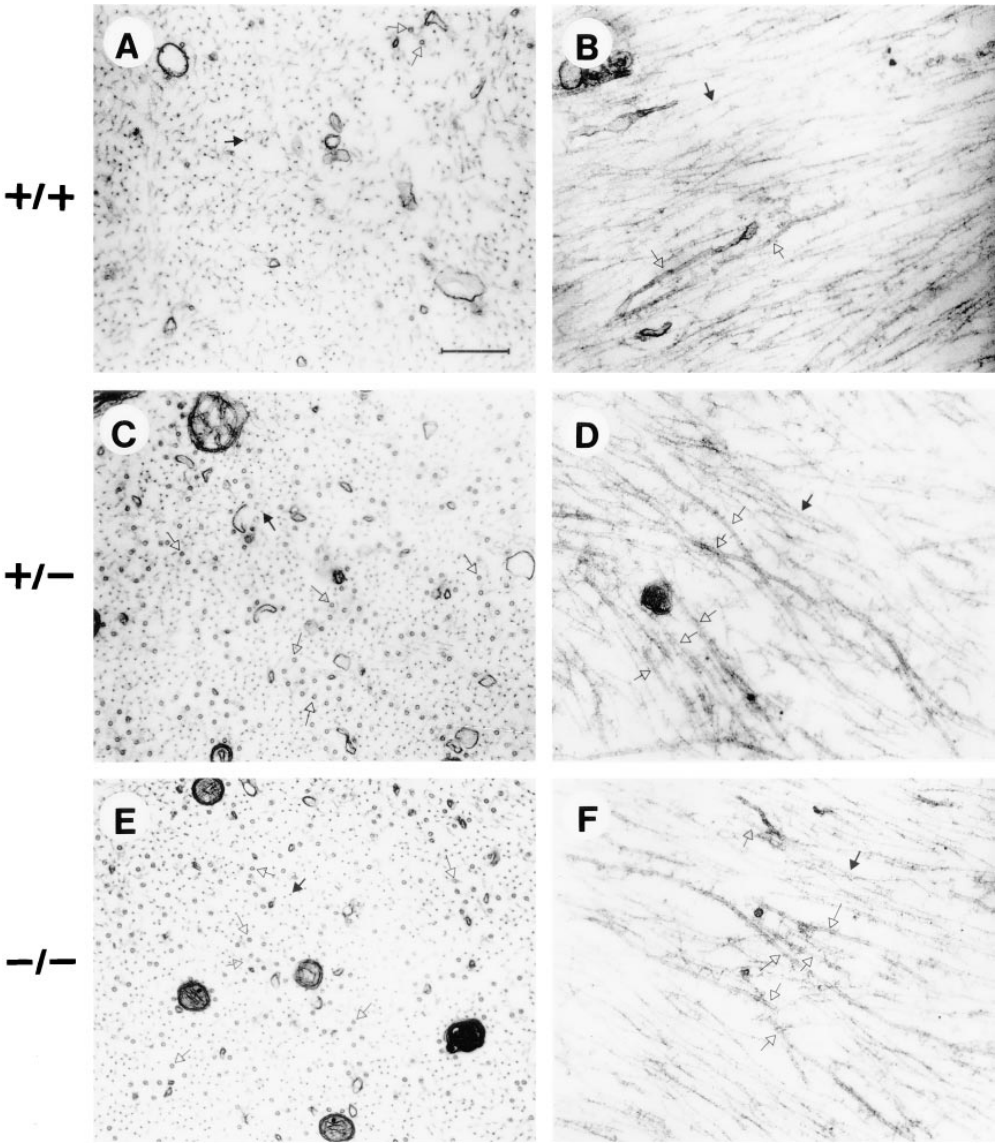

Figure 4. Electron microscopy of ventral root axons. Transverse sections (*A*, *C*, *E*) and longitudinal sections (*B*, *D*, *F*) of myelinated axons >5 mm in diam in the internode from the L5 ventral roots of normal (*A* and *B*) and NF-H +/− (*C* and *D*) and knockout mice (*E* and *F*). The lack of NF-H did not significantly affect the structure of 10-nm neurofilaments. Note, however, a substantial increase in the number of microtubules in both NF-H +/− and −/− mice. *Open arrows*, microtubules; *filled arrows*, 10-nm neurofilaments. Bar, 0.4 μm.

(n = 50) in myelinated axons from control littermates and of 463 ± 94 (n = 58) in the NF-H knockout mice.

Taxol-stabilized cytoskeletal preparations from the sciatic nerve were analyzed to further confirm whether the levels of assembled tubulin were increased. Sciatic nerves between DRG and obturator tendon were dissected and homogenized in taxol/Triton X-100 extraction buffer as described previously (Black et al., 1986). After 30 min at room temperature, the homogenates were centrifuged at 45,000 *g* for 45 min. The pellets were dissolved in 1% SDS–Tris buffer (50 mM Tris, pH 7.4) and the proteins fractionated on SDS-PAGE. As shown on the Coomassie blue–stained gel of these cytoskeletal preparations and corresponding histograms in Fig. 5, the levels of assembled tubulin was increased of ~2.5-fold in samples from the NF-H knockout mice as compared with normal mice. The rise in assembled microtubules in axons lacking NF-H was not due to an increase of total tubulin levels in the sciatic nerve (Fig. 1 *D*) implying that the absence of NF-H contributed to increase the stability of microtubules. We examined by immunoblotting using the TAU-1 antibody whether the levels of tau, a microtubule-associated protein (MAP) that suppresses microtubule dynamics, were altered in the sciatic nerve of NF-H −/− mice. No changes in levels of tau were evident in samples from total nerve extracts (data not shown). However, the TAU-1 antibody detected elevated levels of low molecular weight tau in cytoskeletal preparations from the sciatic nerve of NF-H −/− mice (Fig. 6). From these results, it is possible that NF-H could affect microtubule stability through competition with tau. Thus, a depletion of NF-H levels might yield more binding sites for tau on the surface of microtubules resulting into extra stabilization of axonal microtubules.

Increased Velocity of Neurofilament Transport in Absence of NF-H

Since overexpression of mouse or human NF-H genes in transgenic mice slowed axonal transport of neurofilaments (Collard et al., 1995; Marszalek et al., 1996), we examined

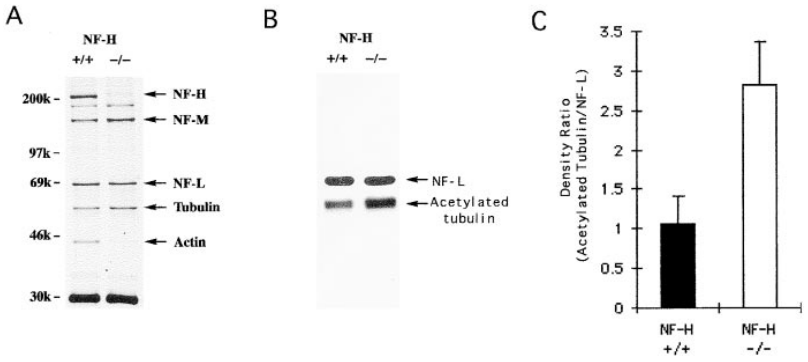

Figure 5. Increase of assembled tubulin in mice lacking NF-H. Taxol-stabilized cytoskeletal preparations from the sciatic nerve of normal (+/+) and NF-H knockout (−/−) mice were fractionated on SDS-PAGE. In *A*, the Coomassie blue–stained gels show increased levels of assembled tubulin in the sciatic nerve of NF-H −/− mice as compared with normal mice. *B* shows immunoblots of taxol-stabilized cytoskeletal preparations using antibodies against NF-L and acetylated tubulin. In *C*, the densitometric analysis of the immunoblots of samples from five mice revealed an increase of ~2.5-fold in levels of acetylated tubulin in taxol-stabilized cytoskeletal preparations from the sciatic nerve of the NF-H −/− mice. Note a decreased level of assembled actin in the NF-H homozygous −/− mice as compared with normal mice. The positions of molecular weight markers are indicated at the left.

whether the velocity of axonal transport of NF-L and NF-M proteins would be increased in NF-H–deficient mice. This was done by the injection of [^{35}S]methionine into the L4-L5 spinal cord with subsequent analysis after 30 d of incorporated radioactivity for NF-L and NF-M proteins in 3-mm segments of the sciatic nerve. In normal mice, at 30 d after injection, the peak of incorporated radioactivity for the NF-L and NF-M proteins occurred in the 9-mm segment of the sciatic nerve while the leading edge of radiolabeled neurofilament proteins was found at the 15-mm segment corresponding to a velocity of ~0.5 mm/d (Fig. 7). In contrast, for the NF-H −/− mice, the leading edge of radiolabeled NF-L and NF-M proteins was found at the 21-mm segment implying a velocity of ~0.7 mm/d (Fig. 7 *C*). To facilitate comparison, the signals were quantified by image analysis and converted to percentage of total radioactivity (Fig. 7, *D–F*). Clearly, the peaks of radiolabeled NF-L and NF-M proteins are broadened in the NF-H −/− axons as compared with NF-H +/+ axons. Whereas <5% of radiolabeled NF-L and NF-M proteins were detected in the 15-mm sciatic segment of normal mice, ~25% of newly synthesized NF-L and NF-M migrated to the 15-mm segment in NF-H −/− mice. In contrast, no dramatic changes in the velocity of NF-M and NF-L transport occurred in the NF-H +/− mice (Fig. 7, *B* and *E*).

Relief of Motor Axonopathy Induced by IDPN

IDPN is a toxic agent known to segregate microtubules from neurofilaments resulting in the excessive accumulation of neurofilaments in the proximal part of the axon and with microtubules forming a central grouping in axons (Griffin et al., 1978; Parhad et al., 1988). The availability of NF-H knockout mice provided us a unique opportunity to assess the role of NF-H in axonopathy induced by this neurotoxin. Intoxication of normal mice by IDPN led to the formation of prominent neurofilamentous swellings in proximal axons originating from spinal motor neurons (Fig. 8, *B* and *C*). In contrast, after IDPN treatment, littermates heterozygous (Fig. 8, *E* and *F*) and homozygous (Fig. 8, *H* and *I*) for the NF-H null mutation did not develop such axonal swellings in motor axons.

Electron microscopic studies of transverse sections of the L5 ventral root axons within the DRG, 7 d after IDPN intoxication, revealed the absence of IDPN-induced segregation of microtubules from neurofilaments in NF-H −/− mice (Fig. 9). We conclude from these results that NF-H is a key mediator of motor axonopathy induced by IDPN exposure.

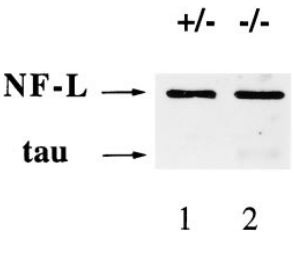

Figure 6. Increased immunodetection of tau protein in cytoskeletal fraction of sciatic nerve from the NF-H knockout mice. After SDS-PAGE, the protein samples described in Fig. 5 were blotted on membrane and treated with alkaline phosphatase. The membrane was then incubated with the TAU-1 antibody (Boehringer Mannheim Corp., Indianapolis, IN) that recognizes hypophosphorylated tau. The sample from the NF-H −/− yielded an increased signal for a band corresponding to low molecular weight tau.

Discussion

Our analysis of NF-H knockout mice provides direct evidence for roles of NF-H protein as a determinant of microtubule density in axons, as a modulator of velocity of neurofilament protein transport in axons and as a key mediator of axonopathy induced by IDPN intoxication. A number of previous reports suggested that neurofilaments can interact between each other and with microtubules via the COOH-terminal domains of NF-H or NF-M but the significance of such interactions has remained elusive (Hisanaga et al., 1990, 1993). The presence of highly charged amino acids in the long tail domains of NF-H also led to the suggestion that this subunit would be implicated as regulator of neurofilament packing density and perhaps control axonal caliber (deWaegh et al., 1992; Hsieh et al., 1994; Nixon et al., 1994). Evidence for this notion has come from studies on the dysmyelinating mutant *Trembler* mouse and on hypomyelinating transgenic mice expressing in Schwann cells either a diphtheria toxin A or SV-40 large T antigen in which reduced levels of NF-H phosphorylation resulted in decreases in axon caliber (deWaegh et al.,

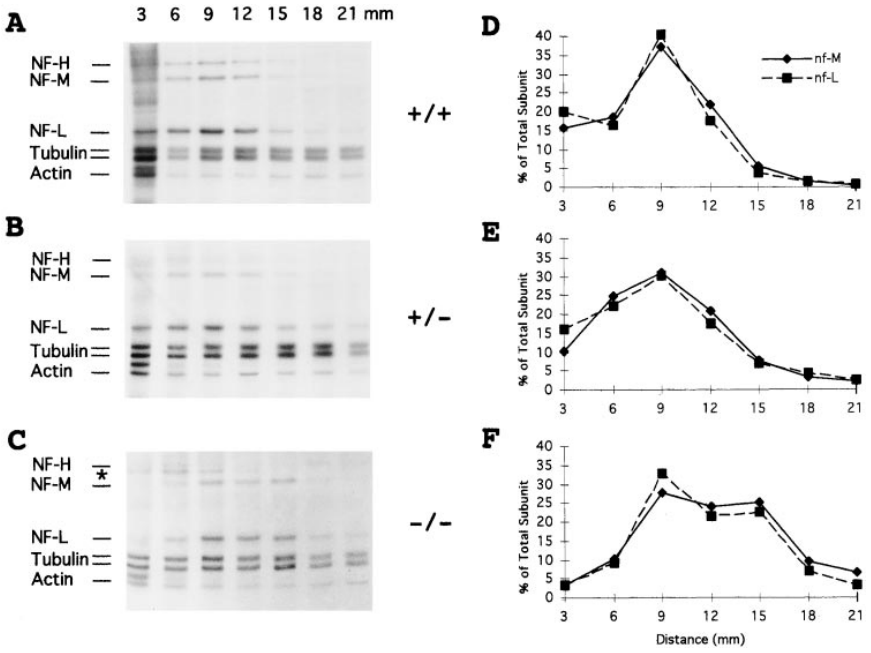

Figure 7. Increased velocity of NF-L and NF-M transport in axons of NF-H–deficient mice. (*A–C*) Fluorographs of slow transport profiles in motor axons of the sciatic nerve from 3-mo-old normal, NF-H +/− and NF-H −/− mice at 30 d after intraspinal injection of [^{35}S]methionine. For each panel, each successive lane represents a 3-mm nerve segment extending distally to the right. (*D–F*) show transport of NF-L and NF-M proteins quantified by densitometry scanning of fluorograph profiles. In the NF-H −/− mice, the leading edge of radiolabeled NF-L and NF-M proteins was detected more distally than in normal mice. No substantial changes of axonal transport occurred in the NF-H +/− mice. The asterisk in *C* points to an ~180-kD band detected in the slow transport component of the sciatic nerve from NF-H −/− mice. The identity of this band remains unclear. The genotyping of mice and immunoblotting of sciatic nerve samples with anti–NF-H antibodies certified that this 180-kD band is not a NF-H species.

1992; Cole et al., 1994). Therefore, as the NF-H subunit is dispensable for the formation of a neurofilament network, it is rather surprising that the disruption of the NF-H gene had so little effects on the spacing density of neurofilaments and caliber of axons. These results can reflect in part the existence of compensatory mechanisms. For instance, it is plausible that an hyperphosphorylation of the NF-M subunit, as revealed by stronger immunodetection signals with the SMI-31 antibody (Fig. 1 *D*), can compensate in part for NF-H function. Unlike NF-H −/− mice, the NF-M −/− mice have decreased levels of NF-L and dramatic reduction of axonal calibers (Elder et al., 1998; our unpublished observations). Therefore, it is clear that the NF-H and NF-M proteins are not playing equivalent roles in neurofilament function. The combined studies with NF-M −/− and NF-H −/− mice indicate that NF-M rather than NF-H protein is a key modulator of axonal caliber.

Another unexpected consequence of NF-H gene disruption was the dramatic increase of ~2.4-fold in the density of microtubules in ventral root axons (Fig. 3 *D*). This was further corroborated by similar increases in levels of assembled acetylated tubulin detected in cytoskeletal preparations from the sciatic nerve (Fig. 5). How could microtubule density in axons be regulated by the NF-H subunit? One possibility, is that the absence of NF-H could somehow increase the rate of axonal transport of tubulin protein or of preassembled microtubules from the cell body. However, the rise in assembled microtubules in NF-H −/− axons was not accompanied by a corresponding increase in the levels of total axonal tubulin (Fig. 1 *D*). This suggests that the lack of NF-H contributed to increase the stability of microtubules. One plausible mechanism by which NF-H could affect microtubule stability is through competition with tau, a microtubule-associated protein (MAP) that suppresses microtubule dynamics (Miyasaka et al., 1993). In vitro binding affinity assays demonstrated that both hypophosphorylated NF-H and tau, compete for similar binding sites on the COOH-terminal region of tubulin (Miyasaka et al., 1993). Therefore, it is conceivable that a depletion of NF-H levels might yield more binding sites for tau on the surface of microtubules resulting into extra stabilization of axonal microtubules. This view is supported by the increased immunodetection of low molecular weight tau with TAU-1 mAb on immunoblots of cytoskeletal preparations from the sciatic nerve of NF-H −/− mice (Fig. 6).

Recent studies with transgenic mice overexpressing murine NF-H led to the suggestion that NF-H can influence the rate of neurofilament transport in axons (Marszalek et al., 1996). The axonal transport studies shown here are consistent with this view. The absence of NF-H increased the velocity of axonal transport of NF-M and NF-L proteins by ~0.2 mm/d (Fig. 7). While this is not a trivial change, this is much less than an eightfold change of velocity suggested by studies of slow axonal transport during development (Willard and Simon, 1983). The exact molecular mechanism by which NF-H can affect neurofilament transport remains unknown. It has been proposed that the NF-H could shift an equilibrium toward assembly of stationary neurofilaments. The effect of NF-H on the mobility of neurofilament proteins could be indirect. The NF-M and NF-H proteins can compete for heterodimer formation with NF-L (Athlan and Mushynski, 1997). Overexpressing NF-H provoked decreases in NF-M levels (Collard et al., 1995; Marszalek et al., 1996) while the absence of NF-H levels resulted in a ~20% increase in NF-M levels. Therefore, one possibility is that changes in levels NF-H affect the levels of NF-M which in turn could be a key regulator of NF-L transport. Future axonal transport studies

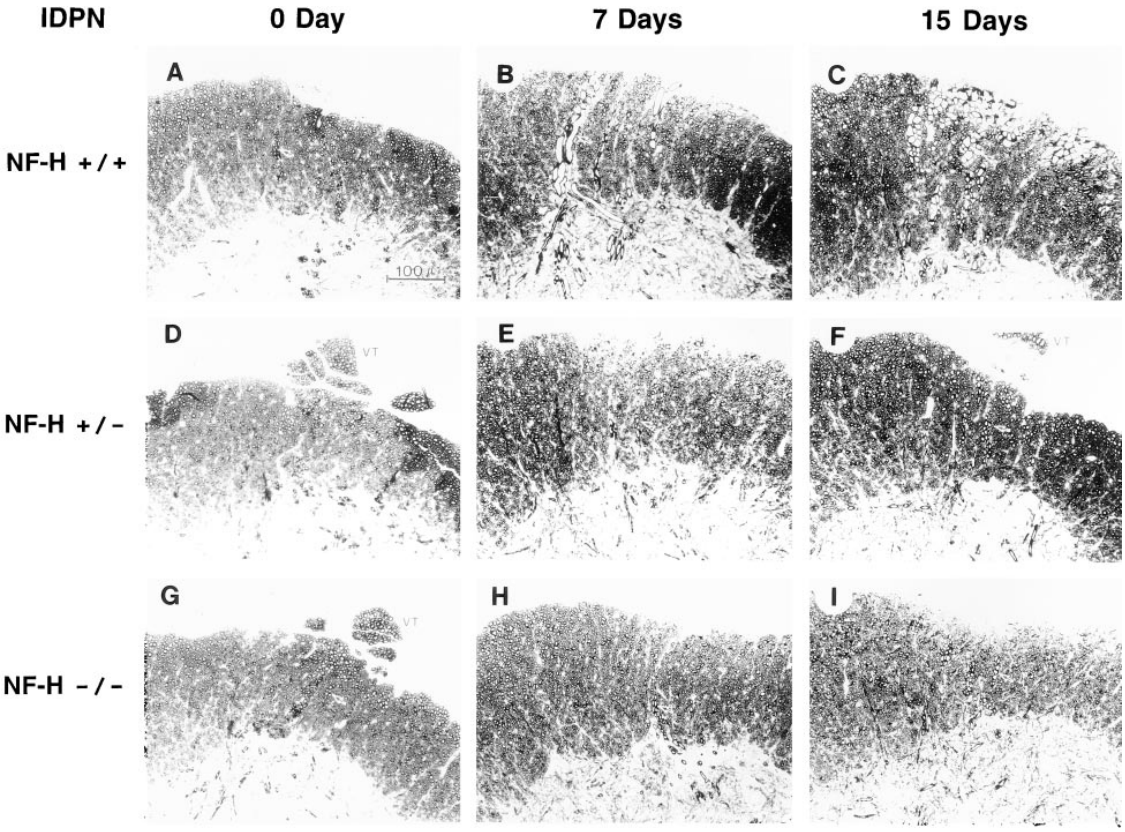

Figure 8. Relief of motor axonopathy resulting from IDPN intoxication in mice lacking NF-H protein. Light micrographs show the anterior horn of the L5 spinal cord in control (*A–C*), NF-H heterozygous +/− (*D–F*) and homozygous −/− mice (*G–I*) at 0 d (*A*, *D*, *G*), 7 d (*B*, *E*, *H*), and 15 d (*C*, *F*, *I*) after IDPN treatment. Note the ventral root axons within the spinal cord are enlarged at 7 d and reach massive proportions at 15 d after IDPN intoxication only in normal mice (*B* and *C*) but not in the NF-H +/− (*E* and *F*) and −/− mice (*H* and *I*). *Open arrows*, the ventral root axons within the spinal cord; *VT*, ventral root axons. Bar, 100 μm.

with NF-M knockout mice and double NF-H; NF-M knockout mice should help to verify this hypothesis.

The IDPN intoxication studies described here further support the view that neurofilaments and microtubules are highly interdependent structures and that the NF-H subunit plays a key role in mediating these interactions. It is remarkable that motor axonopathy due to IDPN intoxication was mitigated not only in NF-H −/− mice but also in NF-H +/− mice. Thus, a ~50% decrease in the levels of NF-H protein was sufficient to alter the properties of axonal cytoskeleton and to confer resistance to IDPN intoxication even though little effect was observed in axonal transport. A key role for NF-H as a mediator of IDPN toxicity is consistent with the report of a transient changes in the phosphorylation state of this protein preceding the onset of segregation of neurofilaments from microtubules and neurofilament transport impairment (Tashiro et al., 1994). While NF-H is clearly acting as a key mediator of IDPN-induced axonopathy, other molecules involved in the phenomenon remain to be defined. Some of these factors could be cell-type specific as neurofilamentous swellings were still detectable in DRG sensory axons of both NF-H +/− and NF-H −/− after IDPN treatment while motor axons were exempt of swellings (data not shown).

Our finding that NF-H is a modulator of microtubule density and a key mediator in IDPN-induced axonopathy may be of relevance to neurodegenerative diseases involving cytoskeletal abnormalities. The abnormal neurofilament depositions in perikaya and neuronal processes are frequently observed in neurodegenerative diseases such as ALS (Carpenter, 1968; Chou, 1992; Hirano et al., 1984), Parkinson's disease (Schmidt et al., 1991) and toxic neuronopathies induced by neurotoxin exposure (Asbury and Johnson, 1978; Graham et al., 1984; Griffin et al., 1978; Troncoso, 1992). Transgenic mouse studies provided compelling evidence that a disorganization of the neurofilament network can play a causative role in the selective degeneration of motor neurons (Côté et al., 1993; Xu et al., 1993; Lee et al., 1994). Studies with transgenic mice overexpressing human NF-H led to the suggestion that the toxicity of disorganized neurofilaments is due to a general disruption of axonal transport (Collard et al., 1995). While transport impairment has been interpreted as reflecting a physical block by neurofilament accumulations, the data presented here suggest that changes in NF-H levels can also perturb the dynamics and function of microtubules, which are key organelles of intracellular transport.

It is noteworthy that the lack of NF-H also resulted in a decreased levels of assembled actin in extracts form the sciatic nerve (Fig. 5 *A*). The NF-H protein was recently

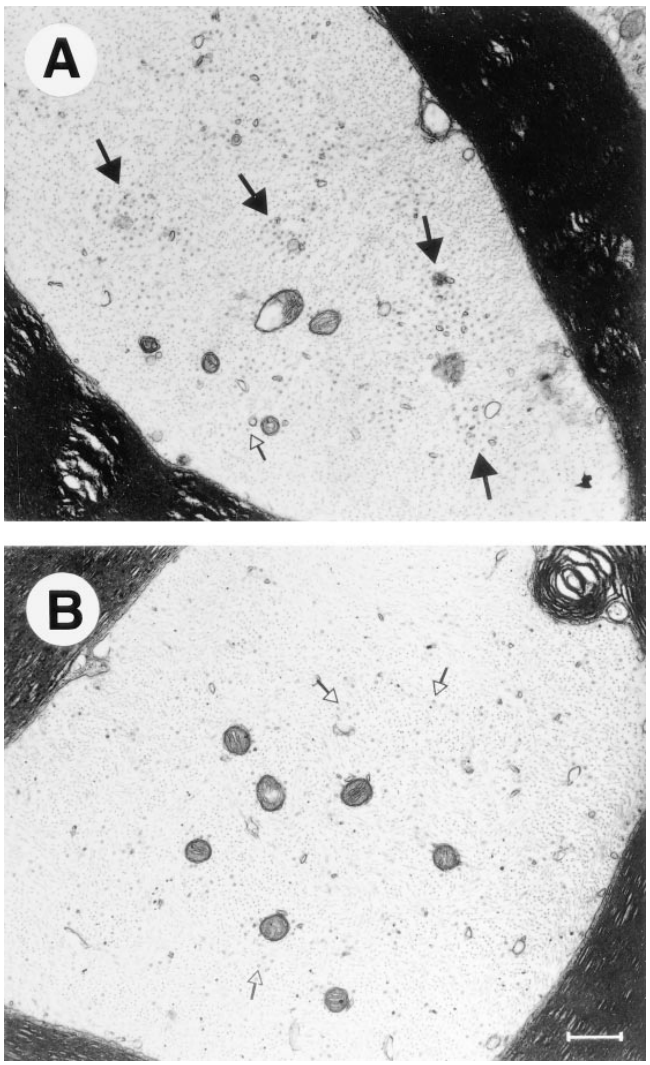

Figure 9. Electron microscopy of transverse sections from the L5 ventral root axons within the DRG after 7 d IDPN treatment in normal littermate +/+ (*A*) and NF-H homozygous −/− mice (*B*). The segregation of microtubules from neurofilament caused by IDPN intoxication is only evident in the control (*A*) as indicated by large filled arrows but not in NF-H homozygous mice (*B*). *Small open arrows*, non-segregated microtubules. Bar, 0.4 μm.

found to be connected to actin filaments in sensory neurons by a linker protein encoded by a neuronal splice form of the BPAG1 gene (Yang et al., 1996), which is responsible for the autosomal recessive *dystonia musculorum*. The large primary sensory axons in BPAG1 knockout mice degenerate within 4 wk after birth, clearly demonstrating that perturbation of the neurofilament-actin connections may have profound effects on axonal integrity. Future breeding studies with the NF-H −/− mice described here will provide a unique approach to assess the in vivo contribution of NF-H protein to BPAG1-mediated degeneration and to other neurodegenerative diseases such as motor neuron disease.

The technical assistance of P. Hince, D. Altshuller, D. Houle, and G. Gagnon is gratefully acknowledged.

This work was supported by the American Health Assistance Foundation and the Amyotrophic Lateral Sclerosis (ALS) Association (USA). Q. Zhu was a recipient of a fellowship from the NeuroScience Network, and J.-P. Julien has a MRC senior scholarship.

Received for publication 5 February 1998 and in revised form 25 June 1998.

References

Asbury, A.K., and P.C. Johnson. 1978. Pathology of Peripheral Nerve: Major Problems in Pathology. Vol. 9. J.L. Bennington, editor. W.B. Saunders, Philadelphia. 311 pp.

Athlan, E.S., and W.E. Mushynski. 1997. Heterodimeric associations between neuronal intermediate filament proteins. *J. Biol. Chem.* 272:31073–31078.

Black, M., P. Keyser, and E. Sobel. 1986. Interval between the synthesis and assembly of cytoskeletal proteins in cultured neurons. *J. Neurosci.* 6:1004–1012.

Carden, M.J., W.W. Schlaepfer, and V.M.-Y. Lee. 1985. The structure, biochemical properties, and immunogenicity of neurofilament peripheral regions are determined by phosphorylation state. *J. Biol. Chem.* 260:9805–9817.

Carpenter, S. 1968. Proximal enlargement in motor neuron diseases. *Neurology.* 18:841–851.

Carpenter, S., G. Karpati, F. Andermann, and R. Gold. 1974. Giant axonal neuropathy: a clinically and morphologically distinct neurological disease. *Arch. Neurol.* 31:312.

Ching, G., and R. Liem. 1993. Assembly of type IV neuronal intermediate filaments in nonneuronal cells in the absence of preexisting cytoplasmic intermediate filaments. *J. Cell Biol.* 122:1323–1335.

Chomczynski, P., and N. Sacchi. 1987. Single-step method of RNA isolation by acid guanidinium thiocyanate-phenol-chloroform extraction. *Anal. Biochem.* 162:156–159.

Chou, S.M. 1992. Pathology: light microscopy of amyotrophic lateral sclerosis. *In* Handbook of Amyotrophic Lateral Sclerosis. R.A. Smith, editor. Marcel Dekker Inc., New York. 133–181.

Cole, J.S., A. Messing, J.Q. Trojanowski, and V.M.-Y. Lee. 1994. Modulation of axon diameter and neurofilaments by hypomyelinating Schwann cells in transgenic mice. *J. Neurosci.* 14:6956–6966.

Collard, J.-F., F. Côté, and J.-P. Julien. 1995. Defective axonal transport in a transgenic mouse model of amyotrophic lateral sclerosis. *Nature.* 375:61–64.

Côté, F., J.F. Collard, and J.P. Julien. 1993. Progressive neuronopathy in transgenic mice expressing the human neurofilament heavy gene: a mouse model of amyotrophic lateral sclerosis. *Cell.* 73:35–46.

deWaegh, S.M., V.M.-Y. Lee, and S.T. Brady. 1992. Local modulation of neurofilament phosphorylation, axonal caliber, and slow axonal transport by myelinating Schwann cells. *Cell.* 68:451–463.

Elder, G.A., V.L. Friedrich, P. Bosco, C. Kamg, A. Gourov, P.-H. Tu, V.M.-Y. Lee, and R.A. Lazzarini. 1998. Absence of the mid-sized neurofilament subunit decreases axonal calibers, levels of light neurofilament (NF-L), and neurofilament content. *J. Cell Biol.* 141:727–739.

Graham, D.G., G. Szakal-Quin, J.W. Priest, and D.C. Anthony. 1984. In vitro evidence that covalent cross-linking of neurofilaments occurs in gamma-diketone neuropathy. *Proc. Natl. Acad. Sci. USA.* 81:4979–4982.

Griffin, J.W., P.N. Hoffman, A.W. Clark, P.T. Carroll, and D.L. Price. 1978. Slow axonal transport of neurofilament proteins: impairment by β,β′-iminodipropionitrile administration. *Science.* 202:633–635.

Hirano, A., H. Donnenfeld, S. Sasaki, and I. Nakano. 1984. Fine structural observations of neurofilamentous changes in amyotrophic lateral sclerosis. *J. Neuropathol. Exp. Neurol.* 43:461–470.

Hisanaga, S., Y. Gonda, M. Inagaki, A. Ikai, and N. Hirokawa. 1990. Effects of phosphorylation of the neurofilament L protein on filamentous structures. *Cell Regul.* 1:237–248.

Hisanaga, S.-I., S. Yasugawa, T. Yamakawa, E. Miyamoto, M. Ikebe, M. Uchiyama, and T. Kishimoto. 1993. Dephosphorylation of microtubule-binding sites at the neurofilament-H tail domain by alkaline, acid, and protein phosphatase. *J. Biochem.* 113:705–709.

Hoffman, P.N., and R.J. Lasek. 1975. The slow component of axonal transport: Identification of the major structural polypeptides of the axon and their generality among mammalian neurons. *J. Cell Biol.* 66:351–366.

Hsieh, S.-T., G.J. Kidd, T.O. Crawford, Z. Xu, W.-M. Lin, B.D. Trapp, D.W. Cleveland, and J.W. Griffin. 1994. Regional modulation of neurofilament organization by myelination in normal axons. *J. Neurosci.* 14:6392–6401.

Julien, J.-P., and W.E. Mushynski. 1982. Multiple phosphorylation sites in mammalian neurofilament polypeptides. *J. Biol. Chem.* 257:10467–10470.

Julien, J.-P., D. Meyer, D. Flavell, J. Hurst, and F. Grosveld. 1986. Cloning and developmental expression of the murine neurofilament gene family. *Brain Res.* 387:243–250.

Julien, J.-P., F. Cote, L. Beaudet, M. Sidky, D. Flavell, F. Grosveld, and W. Mushynski. 1988. Sequence and structure of the mouse gene coding for the largest neurofilament subunit. *Gene.* 68:307–314.

Kirkpatrick, L.L., and S.T. Brady. 1994. Modulation of axonal microtubule cytoskeleton by myelinating Schwann cells. *J. Neurosci.* 14:7440–7450.

Lee, M.K., Z. Xu, P.C. Wong, and D.W. Cleveland. 1993. Neurofilaments are

obligate heteropolymers in vivo. *J. Cell Biol.* 122:1337–1350.
Lee, M.K., J.R. Marszalek, and D.W. Cleveland. 1994. A mutant neurofilament subunit causes massive, selective motor neuron death: implication for the pathogenesis of human motor neuron disease. *Neuron.* 13:975–988.
Lees, J.F., P.S. Shneidman, S.F. Skuntz, M.J. Carden, and R.A. Lazzarini. 1988. The structure and organization of the human heavy neurofilament subunit (NF-H) and the gene encoding it. *EMBO (Eur. Mol. Biol. Organ.) J.* 7:1947–1955.
Levy, E., R.K.H. Liem, P. D'Eustachio, and N.J. Cowan. 1987. Structure and evolutionary origin of the gene encoding mouse NF-M, the middle-molecular-mass neurofilament protein. *Eur. J. Biochem.* 166:71–77.
Liem, J.K.H., S.-H. Yen, G.D. Salomon, and M.L. Shelanski. 1978. Intermediate filaments in nervous tissues. *J. Cell Biol.* 79:637–645.
Mansour, S.L., K. Thomas, and M. Capecchi. 1988. Disruption of the proto-oncogene int-2 in mouse embryo-derived stem cells: a general strategy for targeting mutations to non-selectable genes. *Nature.* 336:348–352.
Marszalek, J.R., T.L. Williamson, M.K. Lee, Z. Xu, P.N. Hoffman, T.O. Crawford, and D.W. Cleveland. 1996. Neurofilament subunit NF-H modulates axonal diameter by selectively slowing neurofilament transport. *J. Cell Biol.* 135:711–724.
Miyasaka, H., S. Okabe, K. Ishiguro, T. Uchida, and N. Hirokawa. 1993. Interaction of the tail domain of high molecular weight subunits of neurofilaments with the COOH-terminal region of tubulin and its regulation by tau protein kinase II. *J. Biol. Chem.* 268:22695–22702.
Myers, M.N., R.A. Lazzarini, V.M.-Y. Lee, W.W. Schlaepfer, and D.L. Nelson. 1987. The human mid-size neurofilament subunit: a repeated protein sequence and the relationship of its gene to the intermediate filament family. *EMBO (Eur. Mol. Biol. Organ.) J.* 6:1617–1626.
Nagy, A., J. Rossant, R. Nagy, W. Abramow-Newerly, and J. Roder. 1993. Derivation of completely cell culture-derived mice from early-passage embryonic stem cell. *Proc. Natl. Acad. Sci. USA.* 90:8424–8428.
Nixon, R.A., P.A. Paskevitch, R.K. Sihag, and C.Y. Thayer. 1994. Phosphorylation on carboxyl terminus domains of neurofilament proteins in retinal ganglion cell neurons in vivo: Influences on regional neurofilament accumulation, interneurofilament spacing, and axon caliber. *J. Cell Biol.* 126:1031–1046.
Parhad, I.M., E.A. Swedberg, D.I. Hoar, C.A. Krekoski, and A.W. Clark. 1988. Neurofilament gene expression following β,β′-iminodipropionitrile (IDPN) intoxication. *Mol. Brain Res.* 4:293–301.
Ramirez-Solis, R., A. Davis, and A. Bradley. 1993. Gene targeting in embryonic stem cells. *Methods Enzymol.* 225:855–878.
Schmidt, M.L., J.M. Murray, V.M.-Y. Lee, W.D. Hill, A. Wertkin, and J.Q. Trojanowski. 1991. Epitope map of neurofilament protein domains on cortical and peripheral nervous system Lewy bodies. *Am. J. Pathol.* 139:53–65.
Tashiro, T., R. Imai, and Y. Komiya. 1994. Early effects of β,β′iminodipropionitrile on tubulin solubility and neurofilament phosphorylation in the axon. *J. Neurochem.* 63:291–300.
Troncoso, J.C., M.R. Gilbert, and N.A. Muma. 1992. Neurotoxicology: light metals. *In* Handbook of Amyotrophic Lateral Sclerosis. R.A. Smith, editor. Marcel Dekker Inc., New York. 543–558.
Watson, D.F., J.W. Griffin, K.P. Fittro, and P.N. Hoffman. 1989. Phosphorylation-dependent immunoreactivity of neurofilaments increases during axonal maturation and β,β′-iminodipropionitrile (IDPN). *J. Neurochem.* 53:1818–1829.
Willard, M., and C. Simon. 1983. Modulations of neurofilament axonal transport during the development of rabbit retinal ganglion cells. *Cell.* 35:551–559.
Xu, Z., L.C. Cork, J.W. Griffin, and D.W. Cleveland. 1993. Increased expression of neurofilament subunit NF-L produces morphological alterations that resemble the pathology of human motor neuron disease. *Cell.* 73:23–33.
Yang, Y., J. Dowling, Q.-C. Yu, P. Kouklis, D.W. Cleveland, and E. Fuchs. 1996. An essential cytoskeletal linker protein connecting actin filaments to intermediate filaments. *Cell.* 86:655–665.
Zhu, Q., S. Couillard-Després, and J.-P. Julien. 1997. Delayed maturation of regenerating myelinated axons in mice lacking neurofilaments. *Exp. Neurol.* 148:299–316.